

The electronic structure and chemical bonding of hypermetallic Al_5C by *ab initio* calculations and anion photoelectron spectroscopy

Alexander I. Boldyrev

Department of Chemistry, The University of Utah, Salt Lake City, Utah 84112; Department of Chemistry and Biochemistry, Utah State University, Logan, Utah 84322-0300

Jack Simons^{a)}

Department of Chemistry, The University of Utah, Salt Lake City, Utah 84112

Xi Li and Lai-Sheng Wang

Department of Physics, Washington State University, Richland, Washington 99352, and W. R. Wiley Environmental Molecular Sciences Laboratory, Pacific Northwest National Laboratory, MS K8-88, P.O. Box 999, Richland, Washington 99352

(Received 22 March 1999; accepted 22 June 1999)

The chemical structure and bonding of the hypermetallic Al_5C and Al_5C^- species have been studied by photoelectron spectroscopy and *ab initio* calculations. Both $\text{Al}_5\text{C}(\text{C}_{2v}, {}^2A_1)$ and $\text{Al}_5\text{C}^-(\text{C}_{2v}, {}^1A_1)$ are found to have planar structures that can be related to that of the planar square Al_4C^- by adding one Al^+ ion or one Al atom to an edge of the square. The planarity of Al_5C and Al_5C^- can be explained in terms of the structure of their highest occupied molecular orbitals which are ligand five-center one- or two-electron bonding MO, respectively, similar to the orbital responsible for the planarity of Al_4C^- . Four peaks were observed in the photoelectron spectra of Al_5C^- with vertical binding energies of 2.67, 2.91, 3.19, and 4.14 eV which compare well with the 2.68, 2.96, 3.27, and 4.35 eV calculated by the Green function method [$\text{OVGF}/6\text{-}311 + G(2df)$]. The excellent agreement between the calculated and experimental electron affinity and excitation energies allow us to completely elucidate the geometrical and electronic structures of Al_5C^- and suggest the most likely structure for the Al_5C molecule. © 1999 American Institute of Physics. [S0021-9606(99)01035-1]

I. INTRODUCTION

A substantial number of hyperaluminum molecules, Al_3O ,¹⁻⁵ Al_4O ,^{2,3,6} Al_nN ($n=3,4$),^{3,6,7} and Al_nS ($n=3-9$),⁸ which contain ligands larger in number than expected based on the octet rule, have been reported in the literature. We recently investigated two hyperaluminum-carbon molecules: Al_3C ⁹ and Al_4C ¹⁰ and their anions. The Al_4C^- anion was found to be particularly interesting because it contains a tetraordinated planar carbon atom (when averaged over zero-point vibrational motions).

In this article, we report a combined photoelectron spectroscopy (PES) and *ab initio* study of the Al_5C^- and Al_5C species, neither of which have been investigated previously. PES of size-selected anions combined with a laser vaporization cluster source has been proven to be a powerful experimental technique to study the electronic structure of a wide range of novel molecular and cluster species.^{7,11-23} The PES spectra of Al_5C^- revealed four detachment channels, corresponding to detachment to the ground and first three excited states of Al_5C . *Ab initio* calculations were performed for both the anion and neutral, which were found to have C_{2v} symmetry with planar structures. The calculated electron affinity and neutral excitation energies are in good agreement with the experiment, thus allowing us to completely characterize the geometrical and electronic structure of the Al_5C molecule and its Al_5C^- anion.

II. EXPERIMENT

The experiments were performed with a magnetic-bottle time-of-flight (TOF) photoelectron apparatus and a laser vaporization cluster source. Details of the apparatus have been published previously.^{24,25} Briefly, the Al_5C^- clusters were produced by a laser vaporization of an aluminum target with pure helium carrier gas. The carbon impurity in the aluminum target was sufficient to give rise to a series of Al_nC^- clusters. We also used a pressed Al/C target (80/20 atom ratio) to produce the Al_5C^- anions and obtained identical results. The cluster anions from the cluster source were extracted perpendicularly into a TOF mass spectrometer. The Al_5C^- cluster were selected and decelerated before intercepted by a detachment laser beam. For the current investigation, two photon energies from a Nd yttrium-aluminum-garnet (YAG) laser were used, 3.496 (355 nm) and 4.661 eV (266 nm). The measured photoelectron TOF spectra were converted to kinetic energy distribution calibrated by the known spectrum of Cu^- . The electron binding energy spectra were obtained by subtracting the kinetic energy distributions from the photon energies. The electron energy resolution was better than 30 meV for 1 eV electrons.

III. COMPUTATIONAL METHODS

We first optimized the geometries of Al_5C and Al_5C^- employing analytical gradients with polarized split-valence basis sets ($6\text{-}311 + G^*$)²⁶⁻²⁸ using a hybrid method which

^{a)}Electronic mail: simons@chemistry.utah.edu

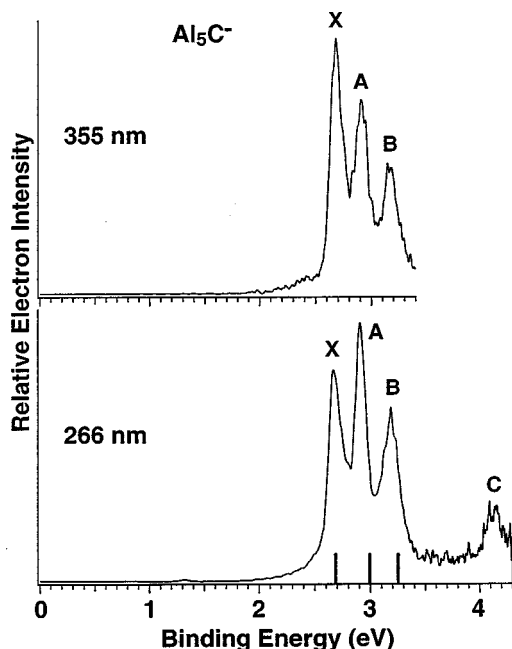


FIG. 1. Photoelectron spectra of Al_5C^- at 355 and 266 nm. The four observed detachment channels are labeled (X, A, B, and C). The vertical lines represent the calculated VDEs from the C_{2v} - Al_5C^- (see Table I).

includes a mixture of Hartree–Fock exchange with density functional exchange–correlation (B3LYP).^{29–31} The energies of the lowest structures thereby identified were refined at the MP2 level of theory.³² Finally, the energies of the lowest structures were refined even further using the CCSD(*T*) level of theory^{33–35} and 6-311+*G*(2*df*) basis sets. The core electrons were kept frozen in treating the electron correlation at the MP2 and CCSD(*T*) levels of theory.

Vertical electron detachment energies from the lowest-energy singlet structures of Al_5C^- were calculated using the outer valence Green function (OVGF) method^{36–40} incorporated in Gaussian-94. The 6-311+*G*(2*df*) basis sets were used in all OVGF calculations, and all calculations were performed using the Gaussian-94 program.⁴¹

IV. EXPERIMENTAL RESULTS

Figure 1 shows the photoelectron spectra of Al_5C^- at 355 and 266 nm. Three major features (X, A, B) were observed in the 355 nm spectrum. One additional feature (C) at

higher binding energy was revealed in the 266 nm spectrum. The lower energy tails in both spectra were due to hot band transitions and were strongly dependent on source conditions. The band widths of the features in the 355 nm spectrum were similar to that in the 266 nm spectrum even though the instrumental resolution was higher at 355 nm than at 266 nm. The relative intensities of the features A and B were enhanced at 266 nm. No vibrational structures were resolved at the higher resolution at 355 nm. The band widths of the spectral features at 355 nm were broader than the instrumental resolution, suggesting that some low-frequency vibrations were excited upon photodetachment and that there was a slight geometry change between the ground state of the anion and the neutral states. The overall spectral features of the Al_5C^- PES spectra were relatively simple, possibly due to the fact that Al_5C^- may have a closed shell electron configuration. A closed shell anion usually gives rise to simpler PES spectra because removal of an electron from each occupied molecular orbital only yields a single spectral feature if there is no orbital degeneracy. As will be shown below from *ab initio* calculations, indeed Al_5C^- is a closed shell anion with a C_{2v} symmetry. The measured adiabatic (ADE) and vertical (VDE) binding energies of the four spectral features are summarized in Table I. The interpretation of each feature will be discussed based on the *ab initio* calculations, which yield detailed information about the structure and bonding of Al_5C^- and Al_5C .

V. THEORETICAL RESULTS

A. The structures of Al_5C^- and Al_5C

In a recent article, we showed that Al_4C^- has an almost planar structure while neutral Al_4C has a tetrahedral structure. The planarization of the anion occurs due to the four-center-one-electron ligand–ligand bond formed by the $1b_{2g}$ -highest occupied molecular orbital (HOMO) in Al_4C^- . The adiabatic electron affinity for Al_4C was found to be 1.93 eV. Based on this information, we speculate that the structures of Al_5C and Al_5C^- can be related to that of Al_4C^- . Specifically, the high electron affinity of Al_4C and the low electronegativity of Al, suggest that the fifth Al atom can donate its valence electron to the $1b_{2g}$ -MO in Al_4C (Al_4C^-), producing the planar Al_4C^- (Al_4C^{2-}), with an Al^+ cation coordinated either to highly electronegative carbon atom above the plane of the Al_4C^- (Al_4C^{2-}) to form a C_{4v} pyra-

TABLE I. Calculated and experimental electron detachment processes and binding energies of Al_5C^- .

State	Experiment VDE(eV)	Experiment ADE(eV)	Structure, C_{2v}		Structure, C_s, II		Structure, C_{4v}		Structure, C_s, I	
			Detachment from MO	Theory, VDE ^a (eV)	Detachment from MO	Theory, VDE ^a (eV)	Detachment from MO	Theory, VDE ^a (eV)	Detachment from MO	Theory, VDE ^a (eV)
X	2.67(3)	2.61(4)	$6a_1$	2.68 (0.86) ^b	$7a'$	2.69 (0.86) ^b	$1b_1$	2.50 (0.87) ^b	$7a'$	2.68 (0.87) ^b
A	2.91(3)	2.82(5)	$5a_1$	2.96 (0.85) ^b	$6a'$	2.88 (0.85) ^b	$2e$	3.28 (0.85) ^b	$6a'$	3.23 (0.85) ^b
B	3.19(3)	3.06(6)	$3b_2$	3.27 (0.84) ^b	$3a''$	3.25 (0.85) ^b	$1b_2$	3.82 (0.85) ^b	$3a''$	3.25 (0.85) ^b
C	4.14(4)	4.04(7)	$2b_2$	4.35 (0.82) ^b	$2a''$	4.30 (0.83) ^b	$4a_1$	3.92 (0.87) ^b	$5a''$	3.51 (0.84) ^b
			$1b_1$	4.78 (0.85) ^b	$5a'$	4.57 (0.85) ^b	$3a_1$	5.74 (0.79) ^b	$2a''$	4.03 (0.84) ^b
			$4a_1$	4.79 (0.80) ^b	$4a'$	4.79 (0.80) ^b			$4a'$	5.73 (0.76) ^b

^aAt the OVGF/6-311+*G*(2*df*) level of theory using MP2/6-311+*G** geometry (see Fig. 2 and Tables II–IV).

^bPole strength is given in parentheses.

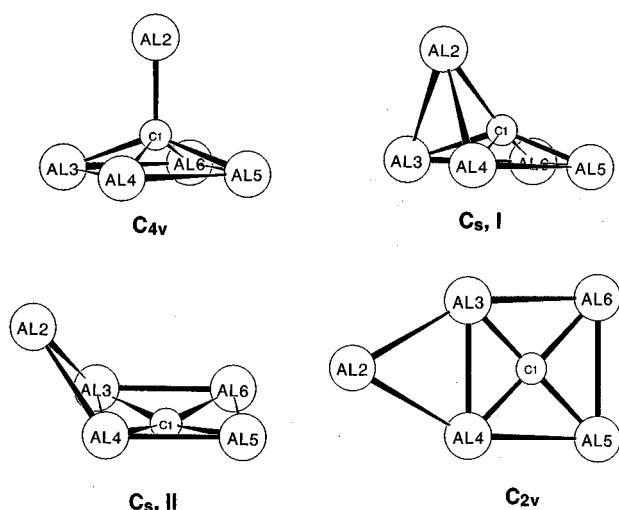


FIG. 2. (a) Optimized Al₅C⁻ and Al₅C structures at the B3LYP/6-311+G* or the MP2/6-311+G* level of theory (see Tables II–IV for parameters).

midal structure for both Al₅C and Al₅C⁻ (the latter having the 1b_{2g}-HOMO of Al₄C²⁻ doubly occupied) or to an edge of the planar square of the Al₄C²⁻ (Al₄C²⁻) to form a planar C_{2v} structure (see Fig. 2).

To test this hypothesis, we first performed geometry optimization for C_{4v} symmetry structures of Al₅C and Al₅C⁻. Both the anion and neutral species should have a b₁-HOMO with Al₅C being a doublet radical and Al₅C⁻ being a closed-shell species. At the B3LYP/6-311+G* level of theory, the C_{4v} symmetry structure of Al₅C⁻ was indeed found to be a minimum with a closed-shell 1a₁²1e⁴2a₁²3a₁²4a₁²1b₂²2e⁴1b₁² valence electron configuration (Fig. 2 and Table II). However, at the MP2/6-311+G* level of theory, this C_{4v}(¹A₁) structure was found to be a second order saddle point. Following its (degenerate) imaginary-frequency distortion, geometry optimization led to a closed-shell C_s, I (¹A', 1a[']2a[']2a[']1a[']23a[']24a[']22a[']25a[']23a[']6a[']27a[']) structure (Fig. 2 and Table III), which is the global minimum at the MP2/6-311+G* level of theory.

The C_{4v} symmetry structure of Al₅C was found to be a second order saddle point at the B3LYP/6-311+G* level of theory with a 1a₁²1e⁴2a₁²3a₁²4a₁²1b₂²2e⁴1b₁² valence electron configuration (Fig. 2 and Table II). Following its (degenerate) imaginary-frequency distortion, geometry optimization led to a closed-shell C_s, I (²A', 1a[']2a[']2a[']1a[']23a[']24a[']22a[']25a[']23a[']6a[']27a[']) structure (Fig. 2 and Table III), which is a local minimum. Unfortunately, at the MP2/6-311+G* level this C_s, I (²A') structure has a very high spin contamination as a result of which we were not able to complete geometry optimization and frequency calculations at this level of theory.

Next, we performed geometry optimization for C_{2v} symmetry planar structures of Al₅C and Al₅C⁻ (Fig. 2 and Table IV). At the B3LYP/6-311+G* level of theory, the C_{2v} symmetry structures of Al₅C⁻ (¹A₁) and Al₅C (²A₁) were indeed found to be global minima with a closed-shell 1a₁²2a₁²1b₂²3a₁²4a₁²1b₁²2b₂²3b₂²5a₁²6a₁² valence electron configuration for the anion and an open shell 1a₁²2a₁²1b₂²3a₁²4a₁²1b₁²2b₂²3b₂²5a₁²6a₁¹ valence electron configuration for the neutral molecule. However, at the MP2/6-311+G* level of theory, this C_{2v}(¹A₁) structure of the anion was found to be a second order saddle point. Geometry optimization within C_s symmetry led to a closed-shell C_s, II (¹A', 1a[']2a[']2a[']1a[']23a[']24a[']22a[']25a[']23a[']6a[']27a[']) structure (Fig. 2 and Table III), which is a local minimum at this level of theory. One can see that the two C_s symmetry structures C_s, I and C_s, II are quite different even though their energies are very close. Their main difference is in the C–Al₂ distance, which is short in the C_s, I structure (i.e., the carbon is pentacoordinated) and is quite long in the C_s, II structure (where carbon is tetraordinated). Unfortunately, at the MP2/6-311+G* level the C_s, II (²A') structure of the neutral species has a very high spin contamination and therefore we were not able to complete geometry optimization and frequency calculations at this level of theory. However, at the B3LYP/6-311+G* and MP2/6-311+G* levels of theory all four structures were found to be very close in energy (Tables II–IV).

To make a more definite conclusion about the global

TABLE II. Calculated molecular properties of the C_{4v}Al₅C⁻ and Al₅C structures.

Al ₅ C ⁻ (C _{4v} , ¹ A ₁)	Al ₅ C ⁻ (C _{4v} , ¹ A ₁)	Al ₅ C (C _{4v} , ² B ₁)	Al ₅ C (C _{4v} , ² B ₁)
B3LYP/6-311+G*	MP2/6-311+G*	B3LYP/6-311+G*	MP2/6-311+G* ^a
E _{tot} = -1250.387 72 a.u.	E _{tot} = -1247.894 22 a.u.	E _{tot} = -1250.303 26 a.u.	E _{tot} = -1247.799 200 a.u.
R(C ₁ –Al ₂) = 1.950 Å	R(C ₁ –Al ₂) = 1.956 Å	R(C ₁ –Al ₂) = 2.010 Å	R(C ₁ –Al ₂) = 2.008 Å
R(C ₁ –Al _{3,4,5,6}) = 2.098 Å	R(C ₁ –Al _{3,4,5,6}) = 2.087 Å	R(C ₁ –Al _{3,4,5,6}) = 2.121 Å	R(C ₁ –Al _{3,4,5,6}) = 2.124 Å
<Al ₂ C ₁ Al _{3,4,5,6} = 110.9°	<Al ₂ C ₁ Al _{3,4,5,6} = 110.2°	<Al ₂ C ₁ Al _{3,4,5,6} = 110.6°	<Al ₂ C ₁ Al _{3,4,5,6} = 110.6°
ν ₁ (a ₁) = 680 cm ⁻¹	ν ₁ (a ₁) = 684 cm ⁻¹	ν ₁ (a ₁) = 604 cm ⁻¹	
ν ₂ (a ₁) = 341 cm ⁻¹	ν ₂ (a ₁) = 353 cm ⁻¹	ν ₂ (a ₁) = 323 cm ⁻¹	
ν ₃ (a ₁) = 182 cm ⁻¹	ν ₃ (a ₁) = 181 cm ⁻¹	ν ₃ (a ₁) = 179 cm ⁻¹	
ν ₄ (b ₁) = 242 cm ⁻¹	ν ₄ (b ₁) = 236 cm ⁻¹	ν ₄ (b ₁) = 193 cm ⁻¹	
ν ₅ (b ₂) = 209 cm ⁻¹	ν ₅ (b ₂) = 233 cm ⁻¹	ν ₅ (b ₂) = 165 cm ⁻¹	
ν ₆ (b ₂) = 116 cm ⁻¹	ν ₆ (b ₂) = 117 cm ⁻¹	ν ₆ (b ₂) = 87 cm ⁻¹	
ν ₇ (e) = 494 cm ⁻¹	ν ₇ (e) = 552 cm ⁻¹	ν ₇ (e) = 377 cm ⁻¹	
ν ₈ (e) = 203 cm ⁻¹	ν ₈ (e) = 226 cm ⁻¹	ν ₈ (e) = 141 cm ⁻¹	
ν ₉ (e) = 34 cm ⁻¹	ν ₉ (e) = 88i cm ⁻¹	ν ₉ (e) = 106i cm ⁻¹	

^aFrequencies were not calculated at this level of theory because of large spin contamination.

TABLE III. Calculated molecular properties of the $C_s, I Al_5C^-$, $C_s, I Al_5C$, and $C_s, II Al_5C^-$ structures.

$Al_5C^- (C_s, I^1A')$	$Al_5C (C_s, I^2A')$	$Al_5C^- (C_s, II^1A')$
MP2/6-311+ G^*	B3LYP/6-311+ G^*	MP2/6-311+ G^*
$E_{tot} = -1247.901\ 675$ a.u.	$E_{tot} = -1250.306\ 353$ a.u.	$E_{tot} = -1247.901\ 35$ a.u.
$R(C_1-Al_2) = 2.099$ Å	$R(C_1-Al_2) = 2.064$ Å	$R(C_1-Al_2) = 3.448$ Å
$R(C_1-Al_{3,4}) = 2.122$ Å	$R(C_1-Al_{3,4}) = 2.077$ Å	$R(C_1-Al_{3,4}) = 1.944$ Å
$R(C_1-Al_{5,6}) = 2.006$ Å	$R(C_1-Al_{5,6}) = 2.123$ Å	$R(C_1-Al_{5,6}) = 2.016$ Å
$\angle Al_2C_1Al_{3,4} = 79.7^\circ$	$\angle Al_2C_1Al_{3,4} = 78.5^\circ$	$\angle C_1Al_3Al_2 = 94.7^\circ$
$\angle Al_2C_1Al_{5,6} = 133.7^\circ$	$\angle Al_2C_1Al_{5,6} = 137.2^\circ$	$\angle Al_3C_1Al_5 = 88.9^\circ$
$\angle Al_3C_1Al_4 = 88.5^\circ$	$\angle Al_3C_1Al_4 = 122.2^\circ$	$\angle Al_3C_1Al_4 = 91.1^\circ$
$\angle Al_5C_1Al_6 = 82.4^\circ$	$\angle Al_5C_1Al_6 = 74.5^\circ$	$\angle Al_5C_1Al_6 = 87.6^\circ$
$\angle Al_3C_1Al_6 = 82.5^\circ$	$\angle Al_3C_1Al_6 = 75.7^\circ$	$\angle Al_3C_1Al_6 = 88.9^\circ$
$\nu_1(a') = 723$ cm $^{-1}$	$\nu_1(a') = 609$ cm $^{-1}$	$\nu_1(a') = 817$ cm $^{-1}$
$\nu_2(a') = 399$ cm $^{-1}$	$\nu_2(a') = 363$ cm $^{-1}$	$\nu_2(a') = 399$ cm $^{-1}$
$\nu_3(a') = 324$ cm $^{-1}$	$\nu_3(a') = 345$ cm $^{-1}$	$\nu_3(a') = 310$ cm $^{-1}$
$\nu_4(a') = 285$ cm $^{-1}$	$\nu_4(a') = 255$ cm $^{-1}$	$\nu_4(a') = 242$ cm $^{-1}$
$\nu_5(a') = 244$ cm $^{-1}$	$\nu_5(a') = 227$ cm $^{-1}$	$\nu_5(a') = 212$ cm $^{-1}$
$\nu_6(a') = 184$ cm $^{-1}$	$\nu_6(a') = 149$ cm $^{-1}$	$\nu_6(a') = 158$ cm $^{-1}$
$\nu_7(a') = 91$ cm $^{-1}$	$\nu_7(a') = 61$ cm $^{-1}$	$\nu_7(a') = 38$ cm $^{-1}$
$\nu_8(a'') = 636$ cm $^{-1}$	$\nu_8(a'') = 558$ cm $^{-1}$	$\nu_8(a'') = 794$ cm $^{-1}$
$\nu_9(a'') = 258$ cm $^{-1}$	$\nu_9(a'') = 281$ cm $^{-1}$	$\nu_9(a'') = 314$ cm $^{-1}$
$\nu_{10}(a'') = 245$ cm $^{-1}$	$\nu_{10}(a'') = 224$ cm $^{-1}$	$\nu_{10}(a'') = 242$ cm $^{-1}$
$\nu_{11}(a'') = 157$ cm $^{-1}$	$\nu_{11}(a'') = 152$ cm $^{-1}$	$\nu_{11}(a'') = 186$ cm $^{-1}$
$\nu_{12}(a'') = 96$ cm $^{-1}$	$\nu_{12}(a'') = 58$ cm $^{-1}$	$\nu_{12}(a'') = 75$ cm $^{-1}$

minimum configuration of Al_5C^- , we performed single point energy calculations of every optimized structure at the CCSD(T)/6-311+ $G(2df)$ level of theory using the MP2/6-311+ G^* optimal geometries. Our results at this level of theory are presented in Table V. The C_{2v} planar structure of Al_5C^- was found to be the global minimum, as was determined at the B3LYP/6-311+ G^* level of theory.

The coordination of the additional Al atom to the edge of Al_4C^- in the C_{2v} structure is favored over the coordination to the central carbon atom in the C_{4v} structure by 3.5 kcal/mol [CCSD(T)/6-311+ $G(2df)$], but essentially all four structures are very close in energy.

B. The low-energy electron detachments

In Table I, we also present results of our OVGf/6-311+ $G(2df)$ calculations of six low lying vertical one-electron detachment processes from the four structures of the Al_5C^- anion. We stress that OVGf results are free from spin contamination and symmetry breaking. One can see that the planar C_{2v} structure has the best agreement with experiment and confirms our assignment of this structure to the global minimum of Al_5C^- . The low-symmetry structure C_s, II also has a good agreement with experiment. We believe that the additional aluminum atom (Al_2) coordinated outside of the

TABLE IV. Calculated molecular properties of the $C_{2v} Al_5C^-$ and Al_5C structures.

$Al_5C^- (C_{2v}, ^1A_1)$	$Al_5C^- (C_{2v}, ^1A_1)$	$Al_5C (C_{2v}, ^2A_1)$	$Al_5C (C_{2v}, ^2A_1)$
B3LYP/6-311+ G^*	MP2/6-311+ G^*	B3LYP/6-311+ G^*	MP2/6-311+ G^{*a}
$E_{tot} = -1250.397\ 414$ a.u.	$E_{tot} = -1247.899\ 770$ a.u.	$E_{tot} = -1250.308\ 653$ a.u.	$E_{tot} = -1247.795\ 113$ a.u.
$R(C_1-Al_2) = 3.868$ Å	$R(C_1-Al_2) = 3.829$ Å	$R(C_1-Al_2) = 4.091$ Å	$R(C_1-Al_2) = 4.089$ Å
$R(C_1-Al_{3,4}) = 1.939$ Å	$R(C_1-Al_{3,4}) = 1.930$ Å	$R(C_1-Al_{3,4}) = 1.985$ Å	$R(C_1-Al_{3,4}) = 1.973$ Å
$R(C_1-Al_{5,6}) = 2.003$ Å	$R(C_1-Al_{5,6}) = 2.006$ Å	$R(C_1-Al_{5,6}) = 1.986$ Å	$R(C_1-Al_{5,6}) = 2.000$ Å
$\angle Al_2C_1Al_{3,4} = 44.6^\circ$	$\angle Al_2C_1Al_{3,4} = 44.9^\circ$	$\angle Al_2C_1Al_{3,4} = 41.6^\circ$	$\angle Al_2C_1Al_{3,4} = 41.5^\circ$
$\angle Al_2C_1Al_{5,6} = 135.0^\circ$	$\angle Al_2C_1Al_{5,6} = 135.2^\circ$	$\angle Al_2C_1Al_{5,6} = 128.6^\circ$	$\angle Al_2C_1Al_{5,6} = 130.0^\circ$
$\nu_1(a_1) = 801$ cm $^{-1}$	$\nu_1(a_1) = 847$ cm $^{-1}$	$\nu_1(a_1) = 751$ cm $^{-1}$	$\nu_1(a_1) = 751$ cm $^{-1}$
$\nu_2(a_1) = 390$ cm $^{-1}$	$\nu_2(a_1) = 400$ cm $^{-1}$	$\nu_2(a_1) = 382$ cm $^{-1}$	$\nu_2(a_1) = 382$ cm $^{-1}$
$\nu_3(a_1) = 289$ cm $^{-1}$	$\nu_3(a_1) = 302$ cm $^{-1}$	$\nu_3(a_1) = 283$ cm $^{-1}$	$\nu_3(a_1) = 283$ cm $^{-1}$
$\nu_4(a_1) = 224$ cm $^{-1}$	$\nu_4(a_1) = 228$ cm $^{-1}$	$\nu_4(a_1) = 211$ cm $^{-1}$	$\nu_4(a_1) = 211$ cm $^{-1}$
$\nu_5(a_1) = 195$ cm $^{-1}$	$\nu_5(a_1) = 205$ cm $^{-1}$	$\nu_5(a_1) = 161$ cm $^{-1}$	$\nu_5(a_1) = 161$ cm $^{-1}$
$\nu_6(a_2) = 74$ cm $^{-1}$	$\nu_6(a_2) = 52$ cm $^{-1}$	$\nu_6(a_2) = 54$ cm $^{-1}$	$\nu_6(a_2) = 54$ cm $^{-1}$
$\nu_7(b_1) = 180$ cm $^{-1}$	$\nu_7(b_1) = 40i$ cm $^{-1}$	$\nu_7(b_1) = 211$ cm $^{-1}$	$\nu_7(b_1) = 211$ cm $^{-1}$
$\nu_8(b_1) = 34$ cm $^{-1}$	$\nu_8(b_1) = 169i$ cm $^{-1}$	$\nu_8(b_1) = 32$ cm $^{-1}$	$\nu_8(b_1) = 32$ cm $^{-1}$
$\nu_9(b_2) = 736$ cm $^{-1}$	$\nu_9(b_2) = 818$ cm $^{-1}$	$\nu_9(b_2) = 693$ cm $^{-1}$	$\nu_9(b_2) = 693$ cm $^{-1}$
$\nu_{10}(b_2) = 310$ cm $^{-1}$	$\nu_{10}(b_2) = 330$ cm $^{-1}$	$\nu_{10}(b_2) = 293$ cm $^{-1}$	$\nu_{10}(b_2) = 293$ cm $^{-1}$
$\nu_{11}(b_2) = 200$ cm $^{-1}$	$\nu_{11}(b_2) = 234$ cm $^{-1}$	$\nu_{11}(b_2) = 148$ cm $^{-1}$	$\nu_{11}(b_2) = 148$ cm $^{-1}$
$\nu_{12}(b_2) = 109$ cm $^{-1}$	$\nu_{12}(b_2) = 124$ cm $^{-1}$	$\nu_{12}(b_2) = 73$ cm $^{-1}$	$\nu_{12}(b_2) = 73$ cm $^{-1}$

^aFrequencies were calculated at this level of theory because of large spin contamination.

TABLE V. Calculated relative energies of the Al_5C^- structures.

$\text{Al}_5\text{C}^-(C_s, \Gamma^1 A')$	CCSD(T)/6-311+G(2df) E_{tot} , a.u.	CCSD(T)/6-311+G(2df) ΔE_{tot} , kcal/mol
$\text{Al}_5\text{C}^-(C_{2v}, \Gamma^1 A_1)$	-1248.049 967	0.00
$\text{Al}_5\text{C}^-(C_s, \Gamma^1 A')$	-1248.047 568	1.51
$\text{Al}_5\text{C}^-(C_s, \Gamma^1 A')$	-1248.046 076	2.44
$\text{Al}_5\text{C}^-(C_{4v}, \Gamma^1 A_1)$	-1248.044 476	3.45

CAI_4 planar fragment can undergo large amplitude out-of-plane motion relative to its position in the planar structure, but that motion does not affect the PES spectra.

The lowest vertical detachment energy (VDE) at this level of theory (2.68 eV) corresponds to removal of an electron from the $6a_1$ -HOMO. The second VDE (2.96 eV) corresponds to electron detachment from the $5a_1$ -MO, the third (3.27 eV) to electron detachment from the $3b_2$ -MO, the fourth (4.35 eV) to electron detachment from the $2b_2$ -MO, and the fifth (4.78 eV) to electron detachment from the $1b_1$ -MO. In all cases, the pole strengths are larger than 0.8; therefore the OVGf method is expected to be valid and all these electron detachments can be considered as primarily one-electron processes. The quantitative picture of the vertical electron detachment energies is in excellent agreement with the peaks in the experimentally observed spectra as illustrated in Fig. 1.

VI. INTERPRETATION OF THE PES SPECTRA

A. Peak X

Removal of an electron from the $6a_1$ -HOMO of Al_5C^- leads to the $C_{2v} \ ^2A_1$ ($1a_1^2 2a_1^2 1b_2^2 3a_1^2 4a_1^2 1b_1^2 2b_2^2 3b_2^2 5a_1^2 6a_1^1$) ground state of Al_5C which, as we calculated, is not very different in geometry from the ground state of Al_5C^- . Therefore, we expect a relatively sharp peak for the X (Al_5C^-) \rightarrow X (Al_5C) transition, which is indeed what is found in the PES spectra of Al_5C^- (peak X in Fig. 1). The calculated vertical (2.68 eV, Table I) electron detachment energy is in excellent agreement with the corresponding experimental peak 2.67 ± 0.03 eV. The $6a_1$ -HOMO (Fig. 3) of Al_5C^- is a pure ligand-ligand bonding MO similar to the $1b_{2g}$ -HOMO in the Al_4C^- anion (see Ref. 10). Coordination of an additional aluminum atom to the four-center-two-electron bond does not destroy the character of this orbital but makes a perturbation resulting in shifting electron density toward the additional aluminum atom. The alternations of the sign of the wave function in the HOMO are, however, preserved.

B. Peak A

The second peak A occurs near 2.91 eV, which is in excellent agreement with the vertical detachment energy 2.96 eV from the $5a_1$ -MO of Al_5C^- at the OVGf/6-311+G(2df) level of theory, resulting in a $C_{2v} \ ^2A_1$ ($1a_1^2 2a_1^2 1b_2^2 3a_1^2 4a_1^2 1b_1^2 2b_2^2 3b_2^2 5a_1^2 6a_1^2$) state of Al_5C . The $5a_1$ -MO is primarily a nonbonding lone pair MO composed of the hybrid $3s, 3p$ -AO of the additional aluminum atom

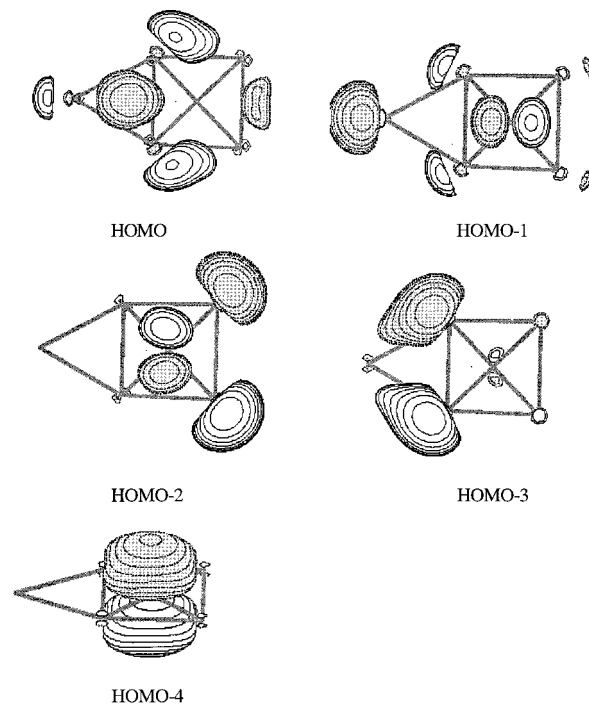


FIG. 3. (a) Molecular orbital pictures (Ref. 42) showing the HOMO ($6a_1$), HOMO-1 ($5a_1$), HOMO-2 ($3b_2$), HOMO-3 ($2b_2$), and HOMO-4 ($1b_1$) of the $C_{2v}\text{Al}_5\text{C}^-$ structure.

with some antibonding central atom–ligand contributions (Fig. 3). The nonbonding nature of the $5a_1$ -MO is consistent with the sharp PES feature.

C. Peak B

The next vertical electron detachment energy (peak B) was found at 3.19 ± 0.03 eV (Table I), which is in excellent agreement with the vertical detachment energy 3.27 eV from the $3b_2$ -MO of Al_5C^- at the OVGf/6-311+G(2df) level of theory, resulting in a $C_{2v} \ ^2B_2$ ($1a_1^2 2a_1^2 1b_2^2 3a_1^2 4a_1^2 1b_1^2 2b_2^2 3b_2^2 5a_1^2 6a_1^2$) state of Al_5C . This MO (Fig. 3) is also a nonbonding lone pair orbital composed primarily of hybrid $3s, 3p$ -AOs of the terminal aluminum atoms with some antibonding central atom–ligand interactions.

D. Peak C

The peak C at 4.14 ± 0.04 eV can be assigned to detachment of an electron from the $2b_2$ -MO (4.35 eV) of Al_5C^- at the OVGf/6-311+G(2df) level of theory, resulting in a $C_{2v} \ ^2B_2$ ($1a_1^2 2a_1^2 1b_2^2 3a_1^2 4a_1^2 1b_1^2 2b_2^2 3b_2^2 5a_1^2 6a_1^2$) state of Al_5C . The $2b_2$ -MO is primarily a nonbonding MO composed of the hybrid $3s, 3p$ -AO of the bridge aluminum atoms with some bonding contributions from the additional aluminum atom (Fig. 3).

VII. DISCUSSION

We synthesized, in the gas phase, two hyperstoichiometric molecules: Al_5C^- and Al_5C for the first time. Four peaks were observed in the photoelectron spectra of Al_5C^- with vertical binding energies of 2.67, 2.91, 3.19, and 4.14 eV which compare well with the 2.68, 2.96, 3.27, and 4.35 eV

calculated by the Green function method [OVGF/6-311+ $G(2df)$]. Overall, we obtained excellent agreement between our experimental and *ab initio* results, allowing us to conclude that the planar structures of Al_5C^- has been established with reasonable certainty. Our results for Al_5C are less certain. Based on the sharp shape of the X-X transition we speculate that both the anion and the neutral species have very similar structures. Also at the B3LYP/6-311+ G^* level of theory the Al_5C (C_{2v} , 2A_1) is a global minimum. Unfortunately, our results at the MP2/6-311+ G^* and the CCSD(T)/6-311+ $G(2df)$ levels of theory are heavily spin-contaminated and therefore are not conclusive. We hope to address this question in the future, but at this point based on the data we have we will consider that Al_5C has the C_{2v} , 2A_1 structure. Both of these species have planar structures with the fifth aluminum cation coordinated to an edge of the planar square structure of the Al_4C^{2-} (Al_4C^-) anion. The planarity of Al_5C and Al_5C^- can be explained by the structure of their HOMOs, which are ligand five-center one- or two-electron bonding MOs, respectively. A similar HOMO is responsible for the planarity of Al_4C^- . Both the anion and neutral species are found to be quite stable: $D_e = 2.24$ eV for Al_5C^- (C_{2v} , 1A_1) \rightarrow Al_4C^- (D_{2d} , 2B_1) + $\text{Al}(^2P)$ and $D_e = 1.62$ eV for Al_5C (C_{2v} , 2A_1) \rightarrow Al_4C (T_d , 1A_1) + $\text{Al}(^2P)$ [all at the CCSD(T)/6-311+ $G(2df)$ levels of theory]. The substantial stability is due to the high degree of ionic character in the bonding between the central atom and the ligands as well as the bonding interactions among the ligand aluminum atoms.

The electron affinity of the Al_5C molecule (2.61 ± 0.04 eV) found in this work is substantially higher than the electron affinity of the pure Al_5 cluster (2.22 ± 0.04 eV).²² Along the $\text{Al}_3\text{C}^- - \text{Al}_4\text{C}^- - \text{Al}_5\text{C}^-$ series, the vertical electron detachment energies range from 2.56 ± 0.06 (Al_3C^-) to 2.65 ± 0.06 eV (Al_4C^-) and then to 2.76 ± 0.03 eV (Al_5C^-).

ACKNOWLEDGMENTS

The theoretical work done in Utah is supported by the National Science Foundation (CHE-9618904). The authors acknowledge the Center for High Performance Computations at the University of Utah for computer time. The experimental work done at Washington is supported by the National Science Foundation (DMR-9622733). We thank Dr. H. Wu for experimental assistance and Dr. V. G. Zakrzewski for help with CCSD(T)/6-311+ $G(2df)$ calculations. The experiment was performed at the W. R. Wiley Environmental Molecular Sciences Laboratory, a national scientific user facility sponsored by DOE's Office of Biological and Environmental Research and located at Pacific Northwest National Laboratory, which is operated for DOE by Battelle under Contract No. DE-AC06-76RLO 1830. L. S. W. is an Alfred P. Sloan Foundation Research Fellow.

¹D. M. Cox, D. J. Trevor, R. L. Whitten, E. A. Rohlfing, and A. Kaldor, *J. Chem. Phys.* **84**, 4651 (1986).

²A. I. Boldyrev and P. v. R. Schleyer, *J. Am. Chem. Soc.* **113**, 9045 (1991).

³V. G. Zakrzewski, W. von Niessen, A. I. Boldyrev, and P. v. R. Schleyer, *Chem. Phys.* **174**, 167 (1993).

- ⁴H. Wu, X. Li, X. B. Wang, C. F. Ding, and L. S. Wang, *J. Chem. Phys.* **109**, 449 (1998).
- ⁵M. F. Jarrold and J. E. Bower, *J. Chem. Phys.* **87**, 1610 (1987).
- ⁶P. v. R. Schleyer and A. I. Boldyrev, *J. Chem. Soc. Chem. Commun.* **21**, 1536 (1991).
- ⁷S. K. Nayak, B. K. Rao, P. Jena, X. Li, and L. S. Wang, *Chem. Phys. Lett.* **301**, 379 (1999).
- ⁸A. Nakajima, T. Taguwa, K. Nakao, K. Hoshino, S. Iwata, and K. Kaya, *J. Chem. Phys.* **102**, 660 (1995).
- ⁹A. I. Boldyrev, J. Simons, X. Li, W. Chen, and L. S. Wang, *J. Chem. Phys.* **110**, 8980 (1999).
- ¹⁰X. Li, L. S. Wang, A. I. Boldyrev, and J. Simons, *J. Am. Chem. Soc.* **121**, 6033 (1999).
- ¹¹J. Fan and L. S. Wang, *J. Phys. Chem.* **98**, 11814 (1994).
- ¹²J. Fan, J. B. Nicholas, J. M. Price, S. D. Colson, and L. S. Wang, *J. Am. Chem. Soc.* **117**, 5417 (1995).
- ¹³H. Wu, S. R. Desai, and L. S. Wang, *J. Chem. Phys.* **103**, 4363 (1995).
- ¹⁴H. Wu, S. R. Desai, and L. S. Wang, *Phys. Rev. Lett.* **76**, 212 (1996).
- ¹⁵L. S. Wang, H. Wu, S. R. Desai, and L. Lou, *Phys. Rev. B* **53**, 8028 (1996).
- ¹⁶H. Wu, S. R. Desai, and L. S. Wang, *J. Am. Chem. Soc.* **118**, 5296 (1996).
- ¹⁷L. S. Wang, H. Wu, and H. Cheng, *Phys. Rev. B* **55**, 12884 (1997).
- ¹⁸L. S. Wang, J. B. Nicholas, M. Dupuis, H. Wu, and S. D. Colson, *Phys. Rev. Lett.* **78**, 4450 (1997).
- ¹⁹S. Li, H. Wu and L. S. Wang, *J. Am. Chem. Soc.* **119**, 7417 (1997).
- ²⁰L. S. Wang, X. B. Wang, H. Wu, and H. Cheng, *J. Am. Chem. Soc.* **120**, 6556 (1998).
- ²¹H. Wu, X. Li, X. B. Wang, C. F. Ding, and L. S. Wang, *J. Chem. Phys.* **109**, 449 (1998).
- ²²X. Li, H. Wu, X. B. Wang, and L. S. Wang, *Phys. Rev. Lett.* **81**, 1909 (1998).
- ²³X. Li and L. S. Wang, *J. Chem. Phys.* **109**, 5264 (1998).
- ²⁴L. S. Wang, H. S. Cheng, and J. Fan, *J. Chem. Phys.* **102**, 9480 (1998).
- ²⁵L. S. Wang and H. Wu, in *Advances in Metal and Semiconductor Clusters, IV. Cluster Materials*, edited by M. A. Duncan (JAI, Greenwich, 1998), pp. 299–343.
- ²⁶A. D. McLean and G. S. Chandler, *J. Chem. Phys.* **72**, 5639 (1980).
- ²⁷T. Clark, J. Chandrasekhar, G. W. Spitznagel, and P. v. R. Schleyer, *J. Comput. Chem.* **4**, 294 (1983).
- ²⁸M. J. Frisch, J. A. Pople, and J. S. Binkley, *J. Chem. Phys.* **80**, 3265 (1984).
- ²⁹R. G. Parr and W. Yang, *Density-Functional Theory of Atoms and Molecules* (Oxford University Press, Oxford, 1989).
- ³⁰A. D. Becke, *J. Chem. Phys.* **96**, 2155 (1992).
- ³¹J. P. Perdew, J. A. Chevary, S. H. Vosko, K. A. Jackson, M. R. Pederson, D. J. Singh and C. Fiolhais, *Phys. Rev. B* **46**, 6671 (1992).
- ³²R. Krishnan, J. S. Binkley, R. Seeger, and J. A. Pople, *J. Chem. Phys.* **72**, 650 (1980).
- ³³J. Cizek, *Adv. Chem. Phys.* **14**, 35 (1969).
- ³⁴G. D. Purvis III and R. J. Bartlett, *J. Chem. Phys.* **76**, 1910 (1982).
- ³⁵G. E. Scuseria, C. L. Janssen and H. F. Schaefer III, *J. Chem. Phys.* **89**, 7382 (1988).
- ³⁶L. S. Cederbaum, *J. Phys. B* **8**, 290 (1975).
- ³⁷W. von Niessen, J. Shirmer, and L. S. Cederbaum, *Comput. Phys. Rep.* **1**, 57 (1984).
- ³⁸V. G. Zakrzewski and W. von Niessen, *J. Comput. Chem.* **14**, 13 (1993).
- ³⁹V. G. Zakrzewski and J. V. Ortiz, *Int. J. Quantum Chem.* **53**, 583 (1995).
- ⁴⁰J. V. Ortiz, V. G. Zakrzewski, and O. Dolgunitcheva, in *Conceptual Trends in Quantum Chemistry*, edited by E. S. Kryachko (Kluwer, Dordrecht, 1997), Vol. 3, p. 463.
- ⁴¹Gaussian 94 (revision A.1). M. J. Frisch, G. M. Trucks, H. B. Schlegel, P. M. W. Gill, B. G. Johnson, M. A. Robb, J. R. Cheeseman, T. A. Keith, G. A. Petersson, J. A. Montgomery, K. Raghavachari, M. A. Al-Laham, V. G. Zakrzewski, J. V. Ortiz, J. B. Foresman, J. Cioslowski, B. B. Stefanov, A. Nanayakkara, M. Challacombe, C. Y. Peng, P. Y. Ayala, W. Chen, M. W. Wong, J. L. Andres, E. S. Replogle, R. Gomperts, R. L. Martin, D. J. Fox, J. S. Binkley, D. J. Defrees, J. Baker, J. J. P. Stewart, M. Head-Gordon, C. Gonzales and J. A. Pople, Gaussian, Inc., Pittsburgh, PA, 1995.
- ⁴²MO pictures were made using MOLDEN3.4 program. G. Schaftenaar, MOLDEN3.4, CAOS/CAMM Center, The Netherlands (1998).